In-vitro apatite formation capacity of a bioactive glass – containing toothpaste

Nasima Kanwal[1], Delia S. Brauer[2], Jonathan Earl[3], Rory M. Wilson[4], Natalia Karpukhina[5], Robert G. Hill[5]

[1]*School of Chemical and Biological Sciences, Queen Mary University of London, London, UK*

[2]*Otto-Schott-Institut, Friedrich-Schiller-Universität, Jena, Germany*

[3]*GlaxoSmithKline Consumer Healthcare, Weybridge, Surrey, KT13 0DE, UK*

[4]*School of Engineering and Materials Science, Queen Mary University of London, London, UK*

[5]*Barts and The London School of Medicine and Dentistry, Queen Mary University of London, London, UK*

Corresponding author details: Natalia Karpukhina, *Dental Physical Sciences, Dental Institute, Barts and The London School of Medicine and Dentistry, Queen Mary University of London, Mile End Road, E1 4NS London, UK,* +44(0)2078825975, +44(0)2078827089, n.karpukhina@qmul.ac.uk

Abstract

Objectives: The *in-vitro* dissolution of bioactive glass-based toothpastes and their capacity to form apatite-like phases in buffer solutions have been investigated.

Materials and Methods: The commercial toothpaste samples were tested on immersion in artificial saliva, Earle's solution and Tris buffer for duration from 10 minutes to four days. The powder samples collected at the end of the immersion were studied using solid-state ^{31}P and ^{19}F nuclear magnetic resonance spectroscopy (NMR), X-ray powder diffraction and Fourier transform infrared (FTIR) spectroscopy. The fluoride concentration in the solution remained after the immersion was measured.

Results: In artificial saliva and in presence of sodium monofluorophosphate (MFP), the bioactive glass and bioactive glass-based toothpastes formed fluoridated apatite-like phases in under 10min. A small amount of apatite-like phase was detected by ^{31}P NMR in the toothpaste with MFP but no bioactive glass. The toothpaste with bioactive glass but no fluoride formed an apatite-like phase as rapidly as the paste containing bioactive glass and fluoride. By contrast, apatite-like phase formation was much slower in Earle's solution than artificial saliva and slower than Tris buffer.

Conclusions: The results of this lab-based study showed that the toothpaste with MFP and bioactive glass formed a fluoridated apatite in artificial saliva and in Tris buffer, as did the mixture of bioactive glass and MFP.

Clinical significance: The presence of fluoride in bioactive glass-containing toothpastes can potential lead to the formation of a fluoridated apatite, which may result in improved clinical effectiveness and durability. However, this should be further tested intra-orally.

Keywords

Sensodyne Repair and Protect®, fluoride toothpaste, bioactive glass, apatite, fluorapatite, sodium monofluorophosphate

Introduction

Enamel, the outer layer of tooth, is formed of 96% (by weight) of an inorganic calcium phosphate mineral called apatite [1], whereas the tooth structure underneath enamel called dentine is less mineralized and consists of by weight 70% hydroxyapatite (HA), 20% organic matter and 10% water [2]. Enamel loss can occur due to a combination of the processes and process of demineralization in the oral conditions is one of them. For example intrinsic and extrinsic acids can cause enamel erosion, whereas acids produced by bacterial action can result in caries [3]. Complete depletion of enamel as a result of aggressive demineralization conditions can expose dentinal tubules and causes tooth sensitivity typically triggered by thermal, osmotic or tactile stimuli including for example hot and cold foods or drinks.

Re-mineralization of enamel occurs by the deposition of ions on the surface from saliva, since enamel has no capability to repair itself as it has no cells. The presence of phosphate and calcium ions in the saliva helps re-mineralization of the enamel [4,5]. In addition, fluorides are well known for their potential to inhibit and repair caries, since fluoridated apatite (FAP) is more resistant to acids. Various toothpastes with added sources of these ions have been developed to help restore partially the lost enamel. Calcium carbonate has been used as an abrasive in toothpaste since the 1850s. It was found that toothpaste with calcium carbonate and fluoride from sodium monofluorophosphate reduces the caries by elevating the level of plaque calcium and hence fluoride [6]. Tschoppe *et al.* [7] have demonstrated that toothpastes containing nano sized HA have higher re-mineralization capacity than amine fluoride toothpaste. Hornby *et al.* [8] have shown that toothpaste containing HA and fluoride in the form of sodium monofluorophosphate significantly reduces acid mediated enamel demineralization and increases re-mineralization compared to fluoride free toothpaste. Vanichvatana *et al.* [9] have reported the re-mineralization effect of fluoride-containing Casein Phosphopeptide Amorphous Calcium Phosphate (CPP-ACP) and beta tricalcium phosphate (β-TCP) and sodium lauryl sulfate. Recent studies have shown that calcium silicate/phosphate-containing toothpaste reduces enamel demineralization and enhances re-mineralization compared to the fluoride and non-fluoride controls [10-12]. This has been attributed to the deposition of calcium silicate on the tooth surface, which releases calcium ions into oral fluids to help nucleate hydroxyapatite. In addition, calcium silicate also buffers the oral fluid by absorbing protons.

Bioactive glass (BAG) was originally invented by Hench as a bone regenerative material. Bioactive glasses form hydroxycarbonated (HCA) apatite following immersion in body fluids. It was discovered later that incorporation of BAG into dentifrices occludes the dentinal tubules and can be useful for the treatment of demineralized teeth and prevent further demineralization [13-15]. A recent report [16] demonstrated the formation of apatite from the commercial bioactive glass-based toothpaste in re-mineralizing media. However, no attempt was made to clarify the type of the apatite formed in presence of a source of fluoride. It is thought that bioactive glass containing toothpaste can form fluoride-substituted apatite in the

presence of soluble fluoride, since fluorine-containing bioactive glasses have been shown to form fluorapatite (FAP) following immersion in Tris buffer and simulated body fluid (SBF) [15]. Therefore, the selection of the immersion media in this study was determined by the previous studies of bioactive glass powders, where typically Tris buffer, SBF or artificial saliva were used for testing. Instead of the SBF solution, the Earl's salt solution with the defined concentration of (bi)carbonate was used. Thus, this selection of the immersion media enabled us to make a direct comparison of the results on the bioactive glass dissolution on its own, in presence of fluoride source and as a part of the toothpaste samples.

The objective of the present study was to investigate the type of apatite formed from the commercial bioactive glass-based toothpaste using the techniques of X-ray diffraction (XRD), Fourier Transformed Infrared (FTIR), ^{31}P and ^{19}F Magic Angle Spinning Nuclear Magnetic Resonance (MAS-NMR) spectroscopy and Inductively Coupled Plasma Optical Emission Spectroscopy (ICP-OES). This is a lab based study conducted in several immersion media. However, the findings of the study are thought to have potential implications for the processes occurring intra-orally on application of the toothpaste. The null hypothesis tested in this lab-based study was that a fluoride free apatite forms as a result of the immersion of the bioactive glass and fluoride containing toothpaste.

Materials and Methods

Fluorapatite formation capacity of Sensodyne Repair and Protect® (SR&P, GlaxoSmithKline, UK) toothpaste (TP) was investigated *in-vitro* using three different buffer solutions; artificial saliva (AS), Tris buffer and Earle's salt solution (ES). This commercial toothpaste contains bioactive glass (NovaMin™) as one of the therapeutic ingredients. Parallel experiments have been carried out for control experimental toothpastes, containing NovaMin™ but no fluoride (NovaMin™ Placebo, TP-BAG) and containing sodium monofluorophosphate (MFP) only (Fluoride Placebo, TP-MFP). The toothpaste samples studied are given in Table 1. In addition to toothpaste samples, NovaMin™ powder (BAG) and a mixture of NovaMin™ powder and MFP (Na_2FPO_3, Sigma Aldrich) (BAG+MFP) were also investigated under the same conditions as the toothpaste samples.

The composition of the AS solution (pH 6.87) is given in Table 2; the solution was supplied by Modus Laboratories Ltd. (Reading, UK). A fresh solution was prepared weekly and stored in the fridge before the use.

Earle's salt solution was prepared by diluting 100 ml of Earle's balanced salt solution (Sigma Aldrich) 10x to 1 litre with distilled water and supplementing it with 2.2 g of sodium hydrogen carbonate ($NaHCO_3$, Sigma Aldrich). The composition is given in Table 2 and a fresh solution was prepared daily.

Tris buffer was prepared by dissolving 15.090 g of tris(hydroxylmethyl)aminomethane (Sigma Aldrich) in 800 ml of distilled water followed by the addition of 44.2ml of 1M hydrochloric acid (HCl, Sigma Aldrich). Solution was kept at 37°C overnight after which pH was adjusted to 7.30 using HCl and a pH meter (Oakton® pH 11 meter; 35811-71 pH electrode) and solution was filled to 2 litres.

In order to hydrolyse the P-F bond of MFP and release free fluoride-ions to solution each buffer solution was supplemented with 5U/ml of bovine alkaline phosphatase (Sigma Aldrich). This concentration of the alkaline phosphatase was used in a previous study [8].

In immersion experiments, 150 mg of BAG powder or 3 g of toothpaste were dispersed in 100 ml of buffer solution (equivalent to 1.5g/L powder to volume ratio) containing 5U/ml phosphatase. Samples were placed in an orbital shaker at an agitation rate of 60 rpm for various time points from 5 min to 4 days. After removing from the shaker samples were filtered through filter paper on a Buchner funnel using a water vacuum pump. A small volume of solution was filtered through 0.2 µm syringe filters for ion release analysis. Filtered samples were kept at 4 °C. Solid residues were dried in an oven at 37°C and were analysed by ^{31}P and ^{19}F magic angle spinning nuclear magnetic resonance (MAS NMR), X-ray diffraction (XRD) and Fourier transform infrared (FTIR) spectroscopy.

^{31}P and ^{19}F MAS NMR spectra were recorded on a Bruker Avance 600 MHz spectrometer at resonance frequencies of 242.9 MHz and 564.7 MHz respectively. ^{31}P MAS NMR spectra were acquired in a 4 mm o.d.

zirconia rotor at a spinning speed of 12 kHz, with a recycle delay of 60 s. A total of 16 or 32 scans were acquired. The concentrated solution of the orthophosphoric acid H_3PO_4 (85%) was used as reference. ^{19}F MAS NMR spectra were acquired in a 2.5 mm rotor at a spinning speed of 21 kHz. Sodium fluoride 1M aqueous solution producing a sharp signal at -120ppm was used as a secondary reference against $CFCl_3$.

The solid residue X-ray diffraction data were collected on a PANalytical X'Pert Pro diffractometer using Ni filtered Cu-Kα radiation (λ = 1.5418 Å). Data were recorded in a flat plate θ/θ geometry over the 2θ range 2 to 70° at a step width of 0.0334° with a count time of 200 s per step. Data were calibrated using an external LaB_6 standard. FTIR spectra were recorded on a Perkin Elmer spectrum 65 with an ATR attachment over a frequency range of 500 – 2000 cm^{-1}.

Solutions were analysed by inductively coupled plasma optical emission spectroscopy (ICP-OES, Varian Vista-Pro). The amount of F^--ion released into solutions was measured with fluoride-ion selective electrode (Orion pH/ISE meter 710, Orion 9609BNWP electrode). Individual calibration was performed using standard solutions diluted with respective buffer solutions to account for ionic strength. Ion release experiments were done in duplicates, though solid residues of duplicates were combined together to provide sufficient quantity of the samples for the characterisation.

Results

Solid-state NMR

Figures 1-3 show the ^{31}P MAS NMR spectra of the precipitates recovered after immersion of the powder and toothpaste samples in buffer solutions plotted along with non-immersed BAG powder (Figure 1i) and MFP (Figure 1ii). Untreated (non-immersed) BAG powder gave a broad signal with the centre at 8.6 ppm (Figure 1i) corresponding to an amorphous orthophosphate charge balanced with sodium and calcium cations from the BAG composition. The spectrum of the MFP is dominated by the two relatively sharp overlapping features at 6.3 and 3.3 ppm (Figure 1ii).

The spectra for the BAG and BAG+MFP after immersion in AS are presented in Figure 1(iii-viii). The broad signal seen in the original BAG spectrum (Figure 1i) becomes asymmetric and narrows with time after immersion (Figure 1v-vii). A fairly sharp feature at 2.9 ppm first appeared in the spectrum of BAG at 40 min of immersion (Figure 1v) and is assigned to an apatite-like phase. The spectrum for the BAG+MFP is broader than for the BAG alone for the same immersion time (40 min, Figure 1iii), though the signal becomes clearly asymmetric with the position changing to 3ppm at 1 hour of immersion (Figure 1iv). It appears that presence of MFP mixed with BAG powder slows down BAG dissolution at the initial stage. However, the spectrum of the 4 days BAG+MFP (Figure 1viii) is very similar to the 24 hours spectrum of the BAG sample (Figure 1vii) and showed a fairly sharp signal at 2.9 ppm.

The spectra in Figure 2i-vii are for the TP samples recovered after the immersion in AS. The samples recovered after 1 hour immersion (Figure 2iv) showed a broad fairly asymmetric peak with the position at 3.6 ppm. The asymmetry is lost at longer time points (6 hours, Figure 2v) and the full width at half maximum (FWHM) of the peak reduces with time giving a sharp peak at 2.9 ppm, which is assigned as an apatite-like phase. There was very little difference between the spectra for the TP samples with fluoride and TP-BAG containing no fluoride after the immersion (not shown here).

The TP-F after 24 hours of immersion produced a fairly sharp ^{31}P signal with the position at 3.1 ppm interpreted as an apatite-like phase (Figure 2viii). Note the signal-to-noise for this spectrum is poor indicating that a low fraction of the phosphate from the AS and soluble MFP was available in solution for precipitation.

Figure 3 shows the ^{31}P MAS NMR spectra following 24 hours immersion in Tris buffer (i, iii, v) and Earle's salt solution (ii, iv, vi). The spectra show fairly broad peaks at a position between 3 and 4 ppm and clear asymmetry, particularly for the TP-BAG toothpaste and BAG powder (Figure 3i-iv). The appearance of the narrow feature at 3ppm was clearer in the BAG powder immersed in Tris buffer (Figure 3i) than in the ES (Figure 3ii) and other samples (Figure 3iii-vi).

The ^{19}F MAS NMR spectra obtained for the toothpaste and powder samples after the immersion in buffers are given in Figure 4. MFP was the only source of fluoride ions for the studied samples, thus, the ^{19}F signal displayed on some of these spectra (Figure 4v-ix) has resulted from the chemical interaction of the fluoride from the hydrolysed MFP with the apatite-like phase emerging from the BAG. Typical presence of the P-F bonds in the MFP is revealed on the ^{19}F MAS NMR spectrum (Figure 4iv) with the multiple sharp signals around -75ppm. Only minute contribution to the ^{19}F NMR signal from the P-F bond is seen from the spectra of the TP after immersion in Tris (Figure 4v).

Both the BAG+ MFP (Figure 4ix) and TP (Figure 4viii) samples immersed for 4 days in AS reveal a relatively broad feature with the peak position at ca. -104ppm suggesting partial fluoride substitution in apatite. The feature is asymmetric indicating presence of other fluoride-containing species. The chemical shift expected for the fluorapatite is -102ppm [17,18]. The 24 hour spectrum of the TP immersed in AS (Figure vii) shows a broader peak at -106ppm and another peak at -225ppm corresponding to NaF. It is thought the NaF peak is due to a small amount of solution being present after filtering that contains sodium and fluoride ions, which crystallise on drying the sample. In the ^{19}F MAS NMR spectrum of the BAG+ MFP immersed in AS for 1 hour (Figure iii) there is a weak broad signal with a chemical shift of -99ppm. Given the breadth of this peak it is consistent with the formation of a fluoridated apatite. Figure 4 shows the ^{19}F MAS NMR spectrum for the TP-F toothpaste that contains no BAG after immersion in AS for one day (Figure 4ii). There is no evidence of any fluorapatite or fluoridated apatite.

For the TP samples soaked in Tris for 3 days (Figure 4vi) a relatively sharp asymmetric feature can be seen in the spectrum with the position at -102ppm close to the chemical shift expected for fluorapatite. Figure 4 shows the ^{19}F MAS NMR spectra for the TP samples immersed in Earle's solution for 24 hours (Figure 4i). There is no evidence of any fluoridated apatite forming in Earle's solution.

X-ray diffraction

Figure 5 displays the selected XRD patterns obtained for the experimental samples. Small broad diffraction peaks at 30-33 degrees and 26 degrees two theta emerging on the patterns for BAG (Figure 5a) match that for apatite. The strength of the diffraction peaks for apatite increases on increasing the immersion time from 40 min to 4 days. It is also seen that in the presence of MFP (Figure 5b) the diffraction peaks for apatite start emerging at a later time point (4 days, Figure 5b(vii)) compared to the BAG without MFP. The sharp diffraction lines seen for the toothpaste samples (Figure 5c) match that for anatase a crystalline polymorph of TiO_2 (PDF 21-1272) [19]. These diffraction lines dominate XRD patterns of the toothpaste samples. However, small and broad diffraction lines at 30-33 degrees two theta can be distinguished for the TP sample after immersion for 24 hours in AS (Figure 5c(vi)). These were also present after AS in the TB-BAG, but not TP-F, that contains no BAG (both not shown here). The broad peak at about 20-23 degrees

two theta (Figure 5c) corresponds roughly with that for silica gel. This broad peak arises probably largely from an amorphous silica added to the toothpastes as it is present in the TP-F samples.

The XRD patterns from the filtrates from the toothpastes showed no evidence of apatite formation in Tris buffer and Earle's solution (not shown here). However, some evidence for apatite formation has been seen from the XRD pattern for the BAG powder after 24 hours in Tris buffer but not in the Earle's salt solution (not shown here).

FTIR spectroscopy

Figure 6 shows the FTIR spectra of the BAG and BAG+ MFP after immersion in AS (Figures 6a and b) and BAG after immersion in ES (Figure 6c). The FTIR spectrum of the BAG sample immersed in AS for 1 hour (Figure 6a(iv)) shows the presence of a crystalline calcium orthophosphate consistent with apatite formation with transmittance bands at 560 and 605 cm^{-1}. These become clearer for the 24 hours BAG samples (Figure 6a(v)). The spectra in Figure 6a also show progressive reduction of the broad transmittance bands at approximately 900 cm^{-1} with increasing immersion time corresponding to the loss of non-bridging oxygens that are main indications for BAG dissolution. In addition, there is a sharpening of the bands at 1000-1060 cm^{-1} corresponding to calcium orthophosphate formation and condensation re-polymerisation of silanol groups.

Figure 6b shows that up to 1 hour of immersion the spectra are identical to the original BAG spectrum (Figure 6b(1-iv)) indicating that the initial stage of the glass dissolution is slowed slightly in the BAG plus MFP. The spectrum of the 4 days BAG+ MFP (Figure 6b(v)) clearly indicates significant glass dissolution and presence of apatite. Figure 6c presents FTIR spectra for the BAG immersed in ES up to 3 days. The only changes observed from the spectra are a small reduction of the band at 900 cm^{-1} relative to the band at ca. 1020 cm^{-1}. The latter band in the original BAG corresponds to the bridging oxygen stretch in Si-O-Si chains of the glass. From the comparison with the AS samples (Figure 6a) the changes observed in ES (Figure 6c) indicate only partial glass degradation in ES that occurs at a slower rate compared to the AS.

FTIR spectra of the toothpaste samples (not shown here) were identical regardless of the time point and composition since they are dominated by the presence of the additional silica used in the toothpaste formulation.

Ion release data

Figure 7 and Table 3 show the concentration profile of calcium and phosphorus during the immersion study in AS. A prominent decrease in calcium ion concentration of the 4 days sample is observed for all

studied samples including the BAG+MFP. However, reduction in calcium concentration was observed by 6 hours (360 min) in toothpaste samples and BAG powder. Phosphorus concentration in general decreases with time, though this decrease is not substantial. The presence of a large concentration of phosphorus and very small concentration of calcium in the solutions of the longest studied time point indicates that calcium acts as limiting species for the formation of apatite in AS.

Figure 8 presents results of the fluoride concentration measurements in artificial saliva for the TP samples. The initial concentration of fluoride measured in solution was between 40 and 50 ppm. However, with time fluoride concentration gradually reduced and reached about 17ppm after 4 days of immersion.

Discussion

Artificial saliva immersion

FAP is considered to be more resistant to acid attack than HA or carbonated apatite [20,21]. Hornby et al. [8] have shown that toothpaste containing HA and a source of fluoride reduce the demineralisation of enamel caused by acid challenges. Fowler et al. [22] have used dynamic secondary ion mass spectrometry to measure incorporation of fluoride into enamel treated with fluoride-containing toothpaste. In our work the FAP formation capacity of the toothpaste, which has the bioactive glass along with sodium monofluorophosphate (MFP) as a source of fluoride, has been demonstrated. Thus, the initial null hypothesis on formation of fluoride-free apatite in presence of fluoride was rejected. The fluoride and the orthophosphate from the MFP may contribute to the formation of apatite-like phases. Techniques such as XRD, FTIR, ^{31}P and ^{19}F MAS NMR and ICP-OES have been used for the characterisation of apatite formed. The XRD is used to detect formation of crystals, apatite in this case. ^{19}F MAS NMR is an effective technique to distinguish FAP from HA or HCA. FTIR is used to monitor degradation of bioactive glass during immersion in the physiological media. The ICP-OES and F ion release data can be used to calculate percentage FAP formed. The immersion times studied here are much longer than an average toothbrushing time. However, it is thought that due to presence of polyacrylic acid in the toothpaste ingredients the bioactive glass particles would retain on the surface of the tooth and continue function. Additionally, it has to be pointed out that the study presented here was done in static lab-based conditions that do not represent fast changing dynamics of the oral environment. However, based on evidences presented here, it is possible that apatite phase if forming under intra-oral conditions would be a fluoride-substituted apatite.

First, apatite has been clearly seen to emerge from the TP sample after 6 hours of immersion based on ^{31}P MAS NMR spectra. It is likely that an apatite-like phase started to form at an earlier time of immersion of the TP, possibly under 10min, however, it cannot be clearly distinguished from the broad signal of the ^{31}P MAS NMR spectra. The skewing of the broad signal is probably not due to residual glass but may be due to a contribution from octacalcium phosphate (OCP) that is known to precede formation of apatite. A fairly sharp ^{31}P MAS NMR peak centred at 2.9 ppm in the TP samples after 4 days of immersion suggests that apatite is the only phase precipitated from this sample. This is also supported by the XRD patterns, FTIR absorption bands and a decrease in Ca and P content of AS measured by ICP-OES. The P content of AS is 310mg/l and the Ca content is 120mg/l. The P and Ca content measured by ICP-OES in the AS are all lower than this value and both decrease with time with the Ca content going to 2-3mg/l. This indicates that despite the calcium phosphosilicate dissolving, which should potentially increase the Ca and P concentration in solution; the actual observed reduction in both concentrations is likely as a result of precipitation of a calcium phosphate phase, i.e. an apatite-like phase.

^{19}F MAS NMR spectra show formation of fluoridated apatite with no precipitation of calcium fluoride CaF_2 which does form from solution with very high fluoride content glasses [15]. The observed reduction of the fluoride concentration in solution is in agreement with formation of the fluoridated apatite. The fluoride release assuming no precipitation of fluoride as fluoride salts should be approximately 45 ppm based on the weight of MFP added in the TP samples. The fluoride release reaches 45ppm at the first time point which corresponds to the maximum possible fluoride from the Na_2FPO_3 but decreases to 17ppm at the longest time point studied.

The degree of apatite fluoridation can be estimated from the ion release data. Overall concentration of Ca and P from all sources (AS, MFP and BAG) is 440 ppm and 424 ppm respectively. Estimations based on decrease in Ca content shows formation of ≈78% fluoridated apatite, whereas the calculations based on P content correspond to ≈70% of fluoridated apatite. Self consistency of percentage calculated in both ways is an indication of validation of the results, though several assumptions were made while doing these calculations. It is assumed that glass dissolves completely and the possibility of non-stoichiometry in apatite lattice is also ignored. A slightly higher percentage of fluoridated apatite based on Ca content could be due to the possibility of confiscation of calcium by mucin and hence removal from solution during the filtration process before the ion release analysis [23].

Additionally, according to Braun & Jana [24] ^{19}F chemical shift can be related to fluoridation percent of apatite. However, estimation based on the Braun and Jana approach gives less than 30% of fluoridation in apatite for the TP after immersion in AS for 4 days from the ^{19}F signal at -104 ppm. However, the spectrum was clearly asymmetric implying presence of the multiple signals.

Similar isotropic chemical shift, line shape and FWHM for the ^{19}F MAS NMR peaks of BAG + MFP and TP samples after 4 days immersion suggests the formation of similarly fluoridated apatite, though amount of MFP in mixed BAG + MFP was higher than in TP. However, the same amount of the alkaline phosphatase enzyme 5U/ml was used to cleave P–F bond for all samples, which is perhaps one of the limitations of this *in-vitro* study. This concludes that concentration of alkaline phosphatase is another factor which controls the amount of fluoridated apatite formed, since according to Michaelis Mentens [25] model enzyme activity kinetics is often controlled by substrate concentration.

Tris and Earle's salt buffers immersion

Formation of fluoridated apatite from TP after immersion in Tris buffer is observed based on the NMR, XRD and FTIR results. Broad ^{31}P MAS NMR spectra of TP after immersion in ES could be an indication of OCP formation or may correspond to a mixture of phases. However, there is no indication of fluoridated apatite formation in ES from the ^{19}F MAS NMR after 24 hours.

Apatite formation in AS is much faster than in Tris buffer, which in turn shows better apatite formation than in ES. This could be due to presence of Ca and phosphate in AS, which promotes precipitation of apatite even at shorter immersion time and hence accelerates glass dissolution. However, the Earle's salt solution contains a high magnesium content; magnesium is known to suppress apatite nucleation and crystal growth, which may inhibit apatite formation. Additionally, the ES is rich in carbonate which precipitates as calcium carbonate as observed by XRD. This may suggest that probably the formation of calcium carbonate on the glass surface in ES acts as a barrier to glass dissolution. These findings also demonstrate how strong is the effect of the immersion solution composition on the evolution of the material during this type of lab-based bioactivity study.

Conclusions

Within the limitations of this lab-based study, the results obtained provide strong evidence for the toothpaste containing bioactive glass in combination with fluoride from MFP forming a fluoridated apatite in Artificial Saliva (AS). Although experimental evidences are required, it is likely that fluoridated apatite would form intra-orally. The ^{31}P NMR spectra, XRD patterns, FTIR are all consistent with the formation of an apatite, whilst the ^{19}F spectra provide evidence for the formation of a fluoridated apatite and this is supported by the ion release and fluoride ion analysis of the solutions. Studies on BAG combined with MFP also show the formation of a fluoridated apatite.

References

1. A. B. Mann and M. E. Dickinson, in *Monographs in Oral Science*, ed. R. M. Duckworth, 2006, vol. 19, pp. 105-131.
2. M. Goldberg, A. B. Kulkarni, M. Young and A. Boskey, *Frontiers in bioscience (Elite edition)*, 2011, **3**, 711-735.
3. M. E. Barbour and G. D. Rees, *The Journal of clinical dentistry*, 2006, **17**, 88-93.
4. E. I. F. Pearce, Y. M. Dong, L. Yue, X. J. Gao, G. L. Purdie and J. D. Wang, *Community Dentistry and Oral Epidemiology*, 2002, **30**, 61-69.
5. L. Shaw, J. J. Murray, C. K. Burchell and J. S. Best, *Caries Research*, 1983, **17**, 543-548.
6. R. J. M. Lynch and J. M. ten Cate, *International Dental Journal*, 2005, **55**, 175-178.
7. P. Tschoppe, D. L. Zandim, P. Martus and A. M. Kielbassa, *Journal of Dentistry*, 2011, **39**, 430-437.
8. K. Hornby, M. Evans, M. Long, A. Joiner, M. Laucello and A. Salvaderi, *International Dental Journal*, 2009, **59**, 325-331.
9. S. Vanichvatana and P. Auychai, *International Journal of Oral Science*, 2013, **5**, 224-228.
10. S. B. Jones, M. Davies, N. Chapman, R. Willson, K. Hornby, A. Joiner and N. X. West, *Journal of dentistry*, 2014, **42 Suppl 1**, S46-52.
11. A. Joiner, F. Schafer, M. M. Naeeni, A. K. Gupta and D. T. Zero, *Journal of dentistry*, 2014, **42 Suppl 1**, S53-59.
12. A. S. Parker, A. N. Patel, R. Al Botros, M. E. Snowden, K. McKelvey, P. R. Unwin, A. T. Ashcroft, M. Carvell, A. Joiner and M. Peruffo, *Journal of dentistry*, 2014, **42 Suppl 1**, S21-29.
13. L. J. Litkowski, G. D. Hack, H. B. Sheaffer and D. C. Greenspan, *Occlusion of dentin tubules by 45S5 Bioglass (R)*, 1997.
14. US 6338751, 2002.
15. D. S. Brauer, N. Karpukhina, M. D. O'Donnell, R. V. Law and R. G. Hill, *Acta Biomater.*, 2010, **6**, 3275-3282.
16. M. L. B. Anthony, V. M. Esther, E. S. Jonathan and J. R. Julian, *Biomed. Glasses*, 2015, **1**, 41-50.
17. A. Stamboulis, R. G. Hill, R. V. Law and S. Matsuya, *Physics and Chemistry of Glasses*, 2004, **45**, 127-133.
18. R. Hill, A. Calver, S. Skinner, A. Stamboulis and R. Law, in *Bioceramics 18, Pts 1 and 2*, eds. T. Nakamura, K. Yamashita and M. Neo, 2006, vol. 309-311, pp. 305-308.
19. M. Horn, Schwerdt.Cf and E. P. Meagher, *Zeitschrift Fur Kristallographie*, 1972, **136**, 273-281.
20. J. M. Tencate and J. D. B. Featherstone, *Crit. Rev. Oral Biol. Med.*, 1991, **2**, 283-296.

21. S. Takagi, H. Liao and L. C. Chow, *Caries Res.*, 2000, **34**, 281-288.
22. C. E. Fowler, L. Gracia, M. I. Edwards, A. Brown and G. D. Rees, *The Journal of clinical dentistry*, 2009, **20**, 186-191.
23. V. Aina, L. Bertinetti, G. Cerrato, M. Cerruti, G. Lusvardi, G. Malavasi, C. Morterra, L. Tacconi and L. Menabue, *Applied Surface Science*, 2011, **257**, 4185-4195.
24. M. Braun and C. Jana, *Chem. Phys. Lett.*, 1995, **245**, 19-22.
25. L. Michaelis, M. L. Menten, K. A. Johnson and R. S. Goody, *Biochemistry*, 2011, **50**, 8264-8269.

Acknowledgements

The authors acknowledge GlaxoSmithKline Consumer Healthcare for funding this experimental work. Dr Harold Toms from the School of Biological and Chemical Sciences of the Queen Mary University of London is kindly thanked for providing assistance with the NMR experiments.

Table 1. Toothpaste samples studied. Sodium monofluorophosphate Na_2FPO_3 was the fluoride source. Nominal concentration of fluoride and BAG are given.

Sample code	Sample description	Fluoride concentration, ppm	Novamin™ concentration, % w/w
TP	SR&P	1450	5
TP-BAG	NovaMin™ Placebo	0	5
TP-F	Fluoride Placebo	1450	0

Table 2. Composition of the AS and ES solution used.

Ingredients	AS	ES
	g/L	g/L
KCl	2.236	0.400
$CaCl_2 \cdot 2H_2O$	0.441	0.265
KH_2PO_4	1.361	-
$NaH_2PO_4 \cdot H_2O$	-	0.122
NaCl	0.759	6.800
MgSO4	-	0.098
NaHCO3	-	2.200
Mucin (type II)	2.200	-
D-Glucose	-	1.000
Phenol Red(Na)	-	0.011

Table 3. Elemental concentration (ppm) of silicon, calcium and phosphorus in AS at different time points.

Samples	Time, min	Si, ppm	Ca, ppm	P, ppm
TP	10	5.3±1.1	108.0±21.6	349.6±69.9
	20	24.0±4.8	68.8±13.8	303.0±60.6
	40	45.5±9.1	50.8±10.2	243.3±48.7
	60	23.2±4.6	64.3±12.9	283.4±56.7
	180	26.0±5.2	9.3±1.9	260.3±52.1
	360	23.1±4.6	2.5±0.5	300.5±60.1
	1440	55.2±11.0	2.0±0.4	267.8±53.6
	5400	52.9±10.6	6.0±1.2	233.6±46.7
TP-BAG	10	38.0±7.6	62.3±12.5	219.1±43.8
	20	34.7±6.9	40.8±8.2	228.9±45.8
	40	27.1±5.4	12.3±2.5	217.3±43.5
	60	23.2±4.6	22.9±4.6	232.8±46.6
	360	42.2±8.4	11.2±2.2	220.1±44.0
	1440	53.3±10.7	4.3±0.9	211.0±42.2
	5400	38.3±7.7	8.3±1.7	167.7±33.5
BAG	5	4.8±1.0	77.3±15.5	256.2±51.2
	20	5.1±1.0	89.8±18.0	262.2±52.4
	40	8.7±1.7	36.6±7.3	253.4±50.7
	60	11.5±2.3	38.2±7.6	241.3±48.3
	1440	110.8±22.2	4.9±1.0	204.2±40.8
	5400	111.1±22.2	2.8±0.6	196.3±39.3

BAG+MFP	5	19.7±3.9	82.6±16.5	315.9±63.2
	20	5.1±1.0	113.1±22.6	347.9±69.6
	40	7.3±1.5	86.0±17.2	318.6±63.7
	60	5.7±1.1	62.6±12.5	304.3±60.9
	5400	112.5±22.5	3.1±0.6	301.1±60.2

Figure captions

Figure 1. ^{31}P MAS NMR spectra of untreated BAG (i), MFP (ii), BAG+MFP after immersion in AS for 40 min (iii), 1 hour (iv); BAG after immersion in AS for 40 min (v), 1 hour (vi), 24 hours (vii), BAG+ MFP after immersion in AS for 4 days (viii) .

Figure 2. ^{31}P MAS NMR spectra of TP after immersion in AS for 10 min (i), 20 min (ii), 40 min (iii), 1 hour (iv), 6 hours (v), 24 hours (vi) and 4 days (vii) and TP-F toothpaste after immersion in AS for 24 hours (viii).

Figure 3. ^{31}P MAS NMR spectra of the samples treated for 24 hours: BAG powder in Tris (i) and ES (ii); TP-BAG in Tris (iii) and ES (iv); TP in Tris (v) and ES (vi).

Figure 4. ^{19}F MAS NMR of toothpaste and powder samples and after immersion: TP in ES for 24 hours (i); TP-F in AS for 24 hours (ii); BAG+ MFP in AS for 1 hour (iii); MFP (iv); TP in Tris for 24 hours (v); TP in Tris for 3 days (vi); TP in AS for 24 hours (vii); TP in AS for 4 days (viii); BAG+MFP in AS for 4 days (ix).

Figure 5. XRD of BAG (a) and BAG+MFP (b) TP sample (c) after immersion in AS for 5 min (i); 10 min (ii); 20 min (iii); 40 min (iv); 1 hour (v); 24 hours (vi) and 4 days (vii).

Figure 6. FTIR of (a) BAG after immersion in AS for 10 min (i), 20 min (ii), 40 min (iii), 1 hour (iv), 24 hours (v) and 4 days (vi); (b) BAG+ MFP after immersion in AS for 10 min (i), 20 min (ii), 40 min (iii), 1 hour (iv), 4 days (v); (c) BAG (i) after immersion in ES for 15 min (ii), 1 hour (iii), 6 hours (iv), 24 hours (v) and 3 days (vi).

Figure 7. Ion release profile of samples immersed in AS.

Figure 8. Fluoride ion release profile of the TP samples in AS.

Figure 1.

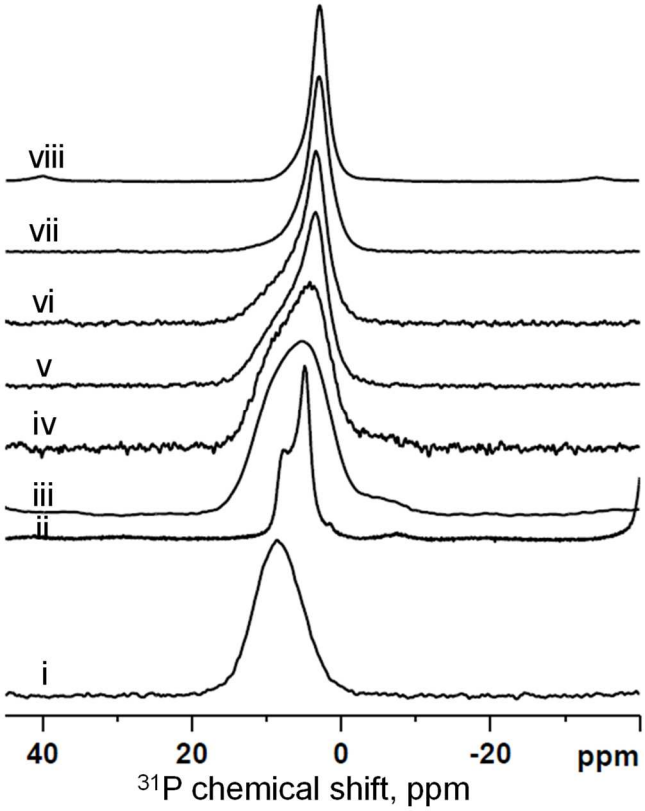

Figure 2.

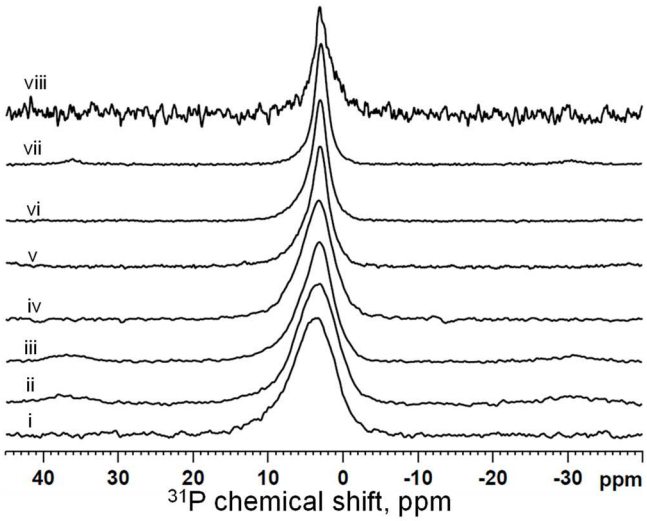
viii
vii
vi
v
iv
iii
ii
i
40
30
20
10
0
-10
-20
-30
ppm
31P chemical shift, ppm

Figure 3.

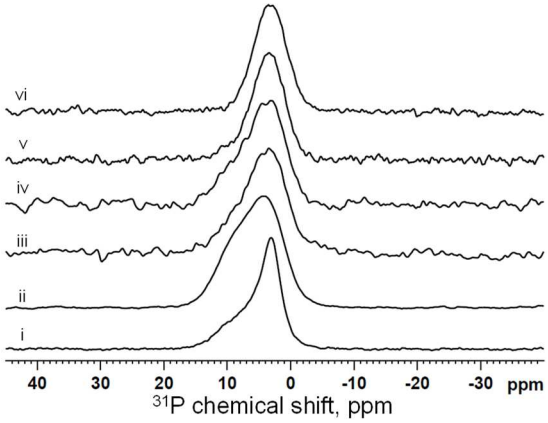

Figure 4.

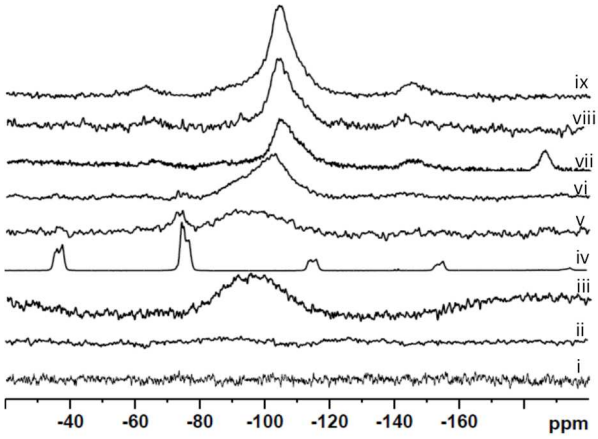

19F chemical shift, ppm

Figure 5.
A

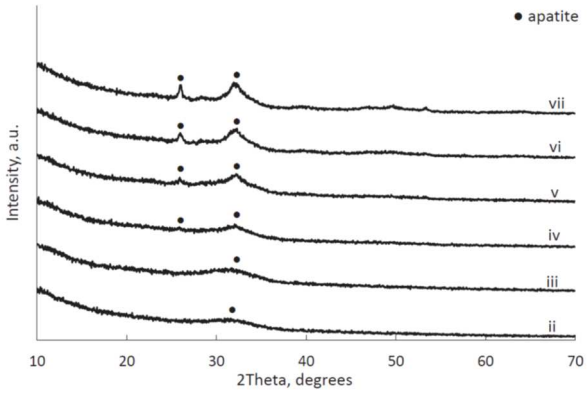
● apatite
vii
vi
v
iv
iii
ii
Intensity, a.u.
10
20
30
40
50
60
70
2Theta, degrees

B

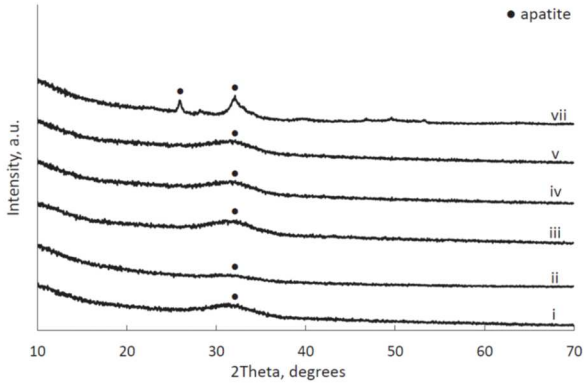
● apatite
vii
v
iv
iii
ii
i
Intensity, a.u.
10
20
30
40
50
60
70
2Theta, degrees

C

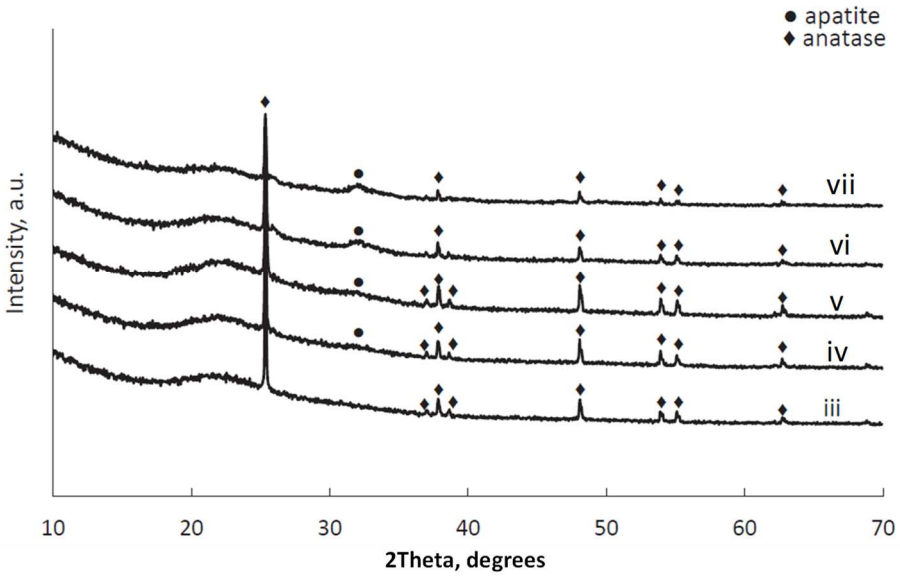
● apatite
♦ anatase
Intensity, a.u.
vii
vi
v
iv
iii
10
20
30
40
50
60
70
2Theta, degrees

Figure 6.
A

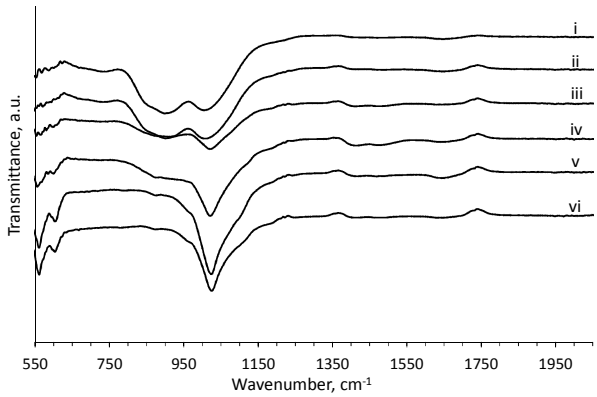
i
ii
iii
iv
v
vi
Transmittance, a.u.
550
750
950
1150
1350
1550
1750
1950
Wavenumber, cm-1

B

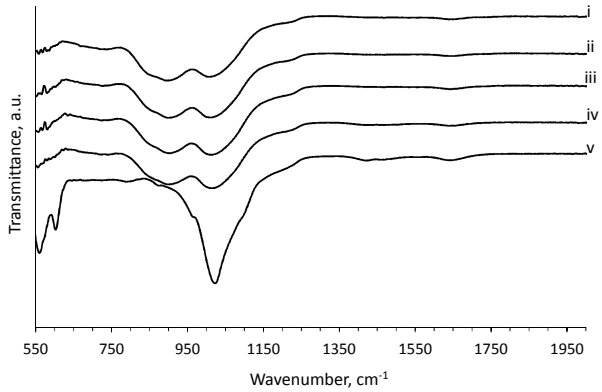
i
ii
iii
iv
v
Transmittance, a.u.
550
750
950
1150
1350
1550
1750
1950
Wavenumber, cm-1

C

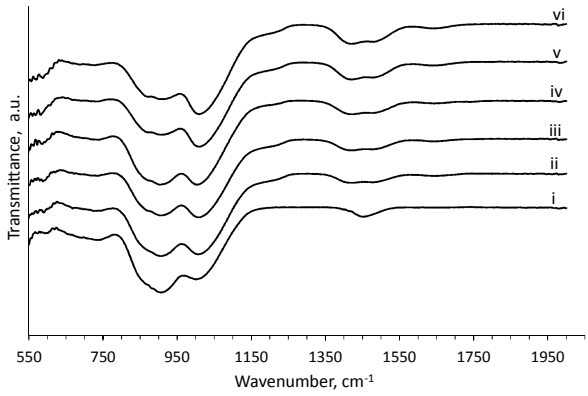
vi
v
iv
iii
ii
i
Transmittance, a.u.
550
750
950
1150
1350
1550
1750
1950
Wavenumber, cm-1

Figure 7.

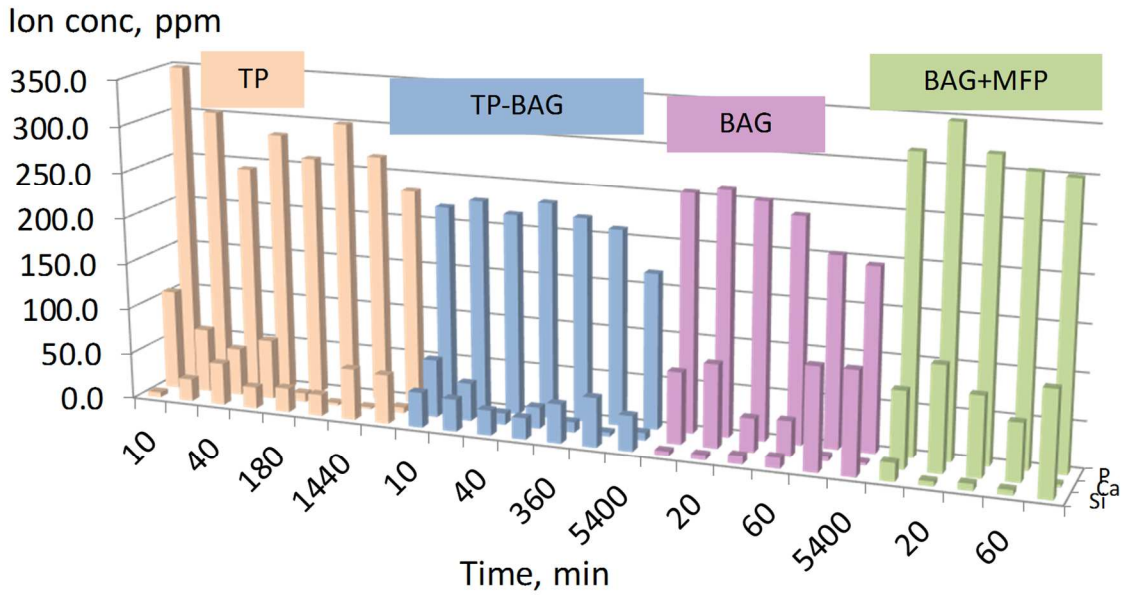
Ion conc, ppm
350.0
300.0
250.0
200.0
150.0
100.0
50.0
0.0
TP
TP-BAG
BAG
BAG+MFP
10
40
180
1440
10
40
360
5400
20
60
5400
20
60
Time, min
P
Ca
Sr

Figure 8.